

From graphs to circuits: Optical heralded generation of N -partite GHZ and W states

Seungbeom Chin*

*International Centre for Theory of Quantum Technologies,
University of Gdańsk, 80-308, Gdańsk, Poland
Department of Electrical and Computer Engineering,
Sungkyunkwan University, Suwon 16419, Korea*

Marcin Karczewski

*International Centre for Theory of Quantum Technologies,
University of Gdańsk, 80-308, Gdańsk, Poland*

Yong-Su Kim†

*Center for Quantum Information, Korea Institute of Science and Technology (KIST), Seoul, 02792, Korea
Division of Nano & Information Technology, KIST School,
Korea University of Science and Technology, Seoul 02792, Korea*

Heralded entanglement generated among identical particles is a useful resource for quantum computations, as heralded schemes distinguish experimental runs producing target states without direct measurement. Nonetheless, these heralded schemes generally entail the incorporation of supplementary particles and modes, thus amplifying the design intricacy. In response to this challenge, a recent work (arXiv:2211.04042) introduced a graph approach for systematic heralded scheme design, which provided several graphical schemes (dubbed “sculpting bigraphs”) for creating multipartite boson entanglement with boson subtractions. However, an indispensable intermediate step remains essential to transmute these sculpting bigraphs into practical heralded entanglement generation circuits: the proposition of heralded subtraction operators (herein dubbed “subtractors”). Assembling the subtractors under the guidance of the sculpting bigraphs, we can seamlessly design heralded schemes for multipartite entangled states. This study establishes a set of translation rules, enabling the mapping of sculpting bigraph elements into linear optical networks through the incorporation of heralded subtractors. Consequently, we devise heralded schemes for the N -partite GHZ state with $2N$ photons, N -partite W state with $2N + 1$ photons, and $N = 3$ Type 5 state (the superposition of $N = 3$ GHZ and W states) with 9 photons. Our results demonstrate that the process of designing heralded schemes for generating entanglement is simplified into the task of searching for suitable sculpting bigraphs.

I. INTRODUCTION

Quantum entanglement is a fundamental phenomenon in quantum mechanics with profound implications in the fields of quantum information and computation science. It is an essential resource for quantum computing [1, 2], quantum cryptography [3], teleportation [4], superdense coding [5], and metrology [6].

In the domain of optics, the predominant and promising approaches for generating entanglement are probabilistic methods leveraging the indistinguishability of photons. The probabilistic entanglement generation methods can be categorized into two distinct types: postselected and heralded schemes. Postselected schemes [7–9], while viable with relatively simple circuits, come with a notable

drawback. In this paradigm, the creation of the target entangled state cannot be confirmed until all the photons are detected, rendering the target state less suitable as a useful resource in quantum information processing. Moreover, Ref. [10] offers evidence that entangling gates with postselection are unable to cover the entire space of multipartite entangled states.

In contrast, the heralded scheme [11–13] adopts a different strategy by incorporating ancillary photons and modes as “heralds” to signal the successful creation of the anticipated target states. This allows for the discrimination of experimental runs that produce the desired target states without directly measuring those states. As a result, the entanglement generated through heralded schemes can be harnessed as a useful resource for quantum computations. However, the heralded schemes generally demand additional particles and modes for the resource of heralding, making them more intricate to design than postselected ones.

* sbthesy@gmail.com

† yong-su.kim@kist.re.kr

To overcome this difficulty for heralded multipartite entanglement generation, a graph approach to heralded entanglement generation is proposed in Ref. [14], providing a systematic strategy to design heralded schemes. Ref. [14] imposed correspondence relations between elements of bipartite graphs (bigraphs) and many-particle systems including boson annihilation operators, which is an extension of the graph picture introduced in Ref. [8] for designing entangled circuits of identical particles with postselection.

Based on the the graph picture, Ref. [14] provided several schemes to generate the multipartite entanglement of bosons with the sculpting protocol [15], which generates an N -partite entangled state by applying tailored $N+K$ single-boson subtraction operators (which is dubbed the *sculpting operator*) with K (≥ 0) ancillary bosons. In the graph picture, all the sculpting operators are represented as bigraphs (which are dubbed *sculpting bigraphs*). By leveraging the advantageous mathematical properties of the graph theory, Ref. [14] has found essential entanglement generation schemes including qubit N -partite GHZ and W states, $N = 3$ Type 5 entangled states (the superposition of $N = 3$ GHZ and W states, see Ref. [16] for the rigorous definition), and qudit N -partite GHZ states.

On the other hand, we need one intermediate step to connect the sculpting bigraphs (which directly correspond to sculpting schemes) with the actual heralded circuits for generating multipartite entanglement: heralded operators for subtracting single bosons from a given many-boson state. Once we know such operators (which we name “subtractors” here), *we can automatically design heralded schemes for multipartite entangled states by assembling the operators according to the guidance of sculpting bigraphs.*

In this study, we demonstrate how to design heralded subtractors employing linear optical elements of polarized photons. Building upon this result, we establish translation rules for mapping sculpting bigraph elements to linear optical systems. By these rules, we can construct linear optical circuits that are the counterparts to any sculpting bigraphs for generating entanglement. Consequently, we devise heralded schemes for the qubit N -partite GHZ state, N -partite W state, and $N = 3$ Type 5 state. Our GHZ generating circuit requires $2N$ photons and W generating one requires $2N + 1$ photons. To the best of our knowledge, these are the smallest numbers of photons required for generating these states with heralding. By combining our results presented here with the graph approach proposed in Ref. [1], the process of designing heralded schemes for generating

entanglement is streamlined into the task of searching for suitable sculpting bigraphs.

II. DIRECTED BIGRAPH MAPPING OF BOSONIC SYSTEMS AND EPM BIGRAPHS

In this section, we review the concept of sculpting protocol [15] and its directed bigraph representation [14]. Among the sculpting bigraphs, we present the definition of their most useful class: effective perfect matching (EPM) bigraphs, directly corresponding to sculpting operators that generate multipartite entanglement in our setup.

A. Sculpting protocol

The sculpting protocol [14, 15] exploits the indistinguishability of identical bosons and spatially overlapped subtraction operators (i.e., a single-boson subtraction operator is a superposition of subtractions on different spatial modes) to generate multipartite entanglement of bosons (see Appendix A of Ref. [14] for a detailed discussion).

In our physical setup, each boson in j th spatial mode ($j \in \{1, 2, \dots, N\}$) has an internal degree of freedom of 2 dimension s ($\in \{0, 1\}$). Therefore boson creation (annihilation) operators are denoted as $\hat{a}_{j,s}^\dagger$ ($\hat{a}_{j,s}$). The sculpting protocol for generating multipartite entanglement consists of three steps for generating multipartite entanglement:

1. Initial state preparation: We prepare a product state of $2N$ bosons in N spatial modes $|Sym_N\rangle$, of which each boson has different states (either spatial or internal) with each other:

$$\begin{aligned} |Sym_N\rangle &\equiv \hat{a}_{1,0}^\dagger \hat{a}_{1,1}^\dagger \hat{a}_{2,0}^\dagger \hat{a}_{2,1}^\dagger \cdots \hat{a}_{N,0}^\dagger \hat{a}_{N,1}^\dagger |vac\rangle \\ &= \prod_{j=1}^N (\hat{a}_{j,0}^\dagger \hat{a}_{j,1}^\dagger) |vac\rangle. \end{aligned} \quad (1)$$

Aside from the state $|Sym_N\rangle$, some sculpting schemes require an ancillary system of K (≥ 0) spatial modes that has a single particle of the same internal state (here we choose 0),

$$\begin{aligned} |Anc_K\rangle &\equiv \hat{a}_{N+1,0}^\dagger \hat{a}_{N+2,0}^\dagger \cdots \hat{a}_{N+K,0}^\dagger |vac\rangle \\ &= \prod_{j=1}^K (\hat{a}_{N+j,0}^\dagger) |vac\rangle. \end{aligned} \quad (2)$$

| Many-particle systems | Directed bipartite Graph $G_b = (U \cup V, E)$ |
|--|--|
| Spatial modes | Labelled vertices (circles, $(j) \in U$) |
| Creation operators | Unlabelled vertices (dots, $\bullet \in V$) with <i>outgoing</i> edges. |
| Annihilation operators | Unlabelled vertices (dots, $\bullet \in V$) with <i>incoming</i> edges |
| Spatial distributions of operators | Directed edges $\in E$ |
| Probability amplitude $\alpha_j^{(l)}$ | Edge weight $\alpha_j^{(l)}$ |
| Internal state $\psi_j^{(l)}$ | Edge weight $\psi_j^{(l)}$ (sometimes replaced with colors) |

TABLE I: Correspondence relations of many-particle systems to directed bipartite graphs

The whole initial state is $|Sym_N\rangle|Anc_K\rangle$ with the main (ancillary) system of N (K) spatial modes, which becomes $|Sym_N\rangle$ when $K = 0$.

2. Operation: To the initial state $|Sym_N\rangle|Anc_K\rangle$, we apply the *sculpting operator*, which is written in the most general form as

$$\begin{aligned}
& \prod_{l=1}^{N+K} \sum_{j=1}^{N+K} (k_{j,0}^{(l)} \hat{a}_{j,0} + k_{j,1}^{(l)} \hat{a}_{j,1}) \\
& \equiv \prod_{l=1}^{N+K} \hat{A}^{(l)} \equiv \hat{A}_{N+K}. \\
& (k_{j,s}^{(l)} \in \mathbb{C} \text{ and } \sum_{j,s} |k_{j,s}^{(l)}|^2 = 1). \quad (3)
\end{aligned}$$

where $\hat{A}^{(l)}$ is a single-boson subtraction operator. The sculpting operator \hat{A}_{N+K} must satisfy a crucial condition: it should eliminate exactly a single particle in each spatial mode. Following Ref. [14], we call it the *no-bunching condition*. It ensures that the resulting overall state $|\Psi\rangle_{fin}$ is composed of states where each spatial mode in the main system contains one boson¹.

3. Final state: We now obtain the final state by calculating

$$|\Psi\rangle_{fin} = \hat{A}_{N+K} |Sym_N\rangle |Anc_K\rangle \quad (4)$$

and verify whether it is genuinely multipartite entangled, i.e., the state cannot be separable under any bipartition of the given system [17].

The main challenge in determining \hat{A}_N for a particular entangled state arises primarily from the no-bunching restriction. As shown in Ref. [14], and to be briefed in the following subsection, the graph method serves as a potent tool to overcome this limitation.

B. Directed graph representation of bosonic systems

In Ref. [14], an undirected bigraph mapping was introduced (Table I of Ref. [14]), which was useful for finding several sculpting schemes in the work. One can consult Appendix A of Ref. [8] for a simple glossary to the graph theory. While the undirected bigraph representation includes all the crucial information on the sculpting operators that can generate entanglement, we need a more comprehensive *directed* bigraph representation to embrace the initial state and the sculpting operator (see Appendix A of Ref. [14]) in the graph presentation. We will explain all our schemes based on the directed bigraph representation in this paper as it has a more direct and intuitive relation with heralded linear optical circuits. In the directed bigraph picture, the complete information on the sculpting protocol from the preparation to the final state is encoded in a graph, which we call a *sculpting directed bigraph*.

Table I enumerates the list of our correspondence relations from fundamental elements of many-boson systems to directed bipartite graphs. In the directed bigraph mapping, both creation and annihilation operators correspond to unlabelled vertices (dots), which are distinguished by the direction of edges attached to them.

¹ Understanding the sculpting schemes with heralded schemes, the boson that remains in the mode contains the

qubit information, while the subtracted boson serves as a heralding.

The initial state $|Sym_N\rangle$ is now drawn as

$$|Sym_N\rangle = \prod_{j=1}^N (\hat{a}_{j,0}^\dagger \hat{a}_{j,1}^\dagger) |vac\rangle = \begin{array}{c} \bullet \rightarrow \textcircled{1} \\ \bullet \dashrightarrow \textcircled{1} \\ \bullet \rightarrow \textcircled{2} \\ \bullet \dashrightarrow \textcircled{2} \\ \vdots \\ \bullet \rightarrow \textcircled{N} \\ \bullet \dashrightarrow \textcircled{N} \end{array} \quad (5)$$

(the internal state edge weights $\{|0\rangle, |1\rangle, |+\rangle = \frac{1}{\sqrt{2}}(|0\rangle + |1\rangle), |-\rangle = \frac{1}{\sqrt{2}}(|0\rangle - |1\rangle)\}$ are denoted as edge colors {Solid Black, Dotted Black, Red, Blue} respectively as in Ref. [14]).

The directed bigraphs present a clear diagrammatic understanding of the following crucial identities

$$\begin{aligned} \forall j \in \{1, 2, \dots, N\}, \\ \hat{a}_{j,\pm} \hat{a}_{j,0}^\dagger \hat{a}_{j,1}^\dagger |vac\rangle &= \pm \hat{a}_{j,\pm}^\dagger |vac\rangle, \\ \hat{a}_{j,+} \hat{a}_{j,-} \hat{a}_{j,0}^\dagger \hat{a}_{j,1}^\dagger |vac\rangle &= 0. \end{aligned} \quad (6)$$

The first identity of Eq. (6) is expressed with directed bigraphs as

$$\begin{array}{c} \bullet \rightarrow \textcircled{j} \xrightarrow{\text{red}} \bullet \\ \bullet \dashrightarrow \textcircled{j} \end{array} = \bullet \xrightarrow{\text{red}} \textcircled{j} \\ \bullet \rightarrow \textcircled{j} \xrightarrow{\text{blue}} \bullet \\ \bullet \dashrightarrow \textcircled{j} \end{array} = -\bullet \xrightarrow{\text{blue}} \textcircled{j} \quad (7)$$

and the second identity as

$$\begin{array}{c} \bullet \rightarrow \textcircled{j} \xrightarrow{\text{red}} \bullet \\ \bullet \dashrightarrow \textcircled{j} \xrightarrow{\text{blue}} \bullet \end{array} = 0. \quad (8)$$

It is worth mentioning that for any $n > 1$

$$\hat{a}_{j,0}^n \hat{a}_{j,0}^\dagger |vac\rangle = \hat{a}_{j,1}^n \hat{a}_{j,1}^\dagger |vac\rangle = 0 \quad (9)$$

corresponds to

$$\begin{array}{c} \bullet \rightarrow \textcircled{j} \xrightarrow{\text{red}} \bullet \\ \bullet \dashrightarrow \textcircled{j} \xrightarrow{\text{blue}} \bullet \end{array} = \begin{array}{c} \bullet \dashrightarrow \textcircled{j} \xrightarrow{\text{red}} \bullet \\ \bullet \dashrightarrow \textcircled{j} \xrightarrow{\text{blue}} \bullet \end{array} = 0 \quad (10)$$

The above identities play an essential role in finding sculpting directed bigraphs for generating genuine entanglement by defining a special type of graphs, i.e., *effective perfect matching (EPM) directed bigraphs* [14].

C. EPM directed bigraphs for generating entanglement

Definition 1. (*EPM directed bigraphs*) If all the edges of a bigraph attach to the circles as one of the following bigraphs

$$\begin{array}{c} \bullet \rightarrow \textcircled{j} \xrightarrow{\text{red}} \bullet \\ \bullet \dashrightarrow \textcircled{j} \xrightarrow{\text{blue}} \bullet \end{array} \quad (a) \quad \begin{array}{c} \bullet \rightarrow \textcircled{j} \xrightarrow{\text{red}} \bullet \\ \bullet \dashrightarrow \textcircled{j} \xrightarrow{\text{blue}} \bullet \end{array} \quad (b) \quad \begin{array}{c} \bullet \dashrightarrow \textcircled{j} \xrightarrow{\text{red}} \bullet \\ \bullet \dashrightarrow \textcircled{j} \xrightarrow{\text{blue}} \bullet \end{array} \quad (c) \quad (11)$$

then it is an *effective perfect matching (EPM) bigraph*.

A crucial property of an EPM bigraph is that the final state by the corresponding sculpting operator is fully determined by the perfect matchings (PMs) of the bigraph (a set of disjoint edges that cover all the vertices in a given bigraph, see Appendix A of Ref. [8]), which we can show using identities (7) and (8) (see Sec. IV of Ref. [14] for the detailed explanation). All the sculpting bigraphs for generating genuine qubit entanglement in Ref. [14] correspond to EPM bigraphs.

Remark 1.— The main system and ancillary system consist of different type of bigraphs in Eq. (11). Bigraph (a) of (11) corresponds to a spatial mode in the main system and (b) or (c) to a spatial mode in the ancillary system. Since the ancillary modes always has the same internal state, we need to choose between (b) and (c). Following the definition of the ancillary system $|Anc_K\rangle$ (2), we set that an EPM bigraph consists of circles of (a) and (b). See Fig. 1 (b) and (c) in which all the vertices are attached to the circles either as (a) or (b).

Remark 2.— Comparing the EPM directed bigraphs in Fig. 1 with the EPM (undirected) bigraphs presented in (20), (27), and (32) of Ref. [14], we can easily see that the RHS of the directed ones in Fig. 1 (a), (b), and (c) without direction are equal to (20), (27), and (32) in Ref. [14]. This is by the fact that the information on the sculpting operators is in the LHS of the directed graphs, which is solely represented in the undirected graphs in Ref. [14].

III. FROM EPM BIGRAPHS TO OPTICAL CIRCUITS

Ref. [14] exploited the special property of EPM bigraphs (Property 2 of Section IV in Ref. [14]) to find

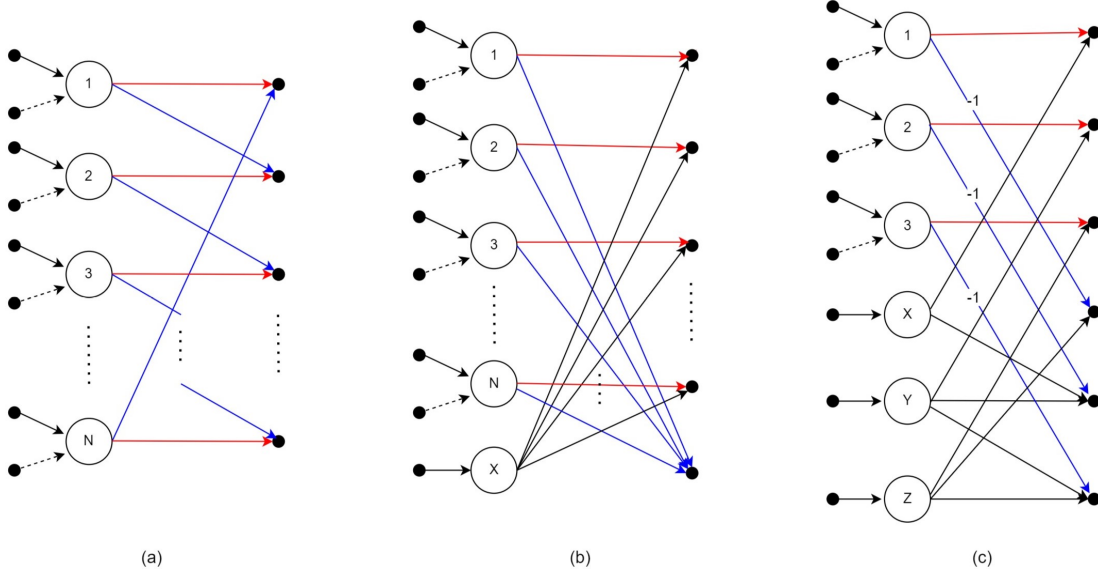


FIG. 1: Three EPM directed bigraphs that corresponds to (a) GHZ-state, (b) W-state, and (c) $N = 3$ Type 5 entangled states (a superposition of $N = 3$ GHZ and W states, see Ref. [16] for a more rigorous definition) introduced in Ref. [14]. Note that the probability amplitude weights are omitted for all of graphs except for the blue edges in (c) that have -1 . This is a simplified notation, in which all the absolute values of probability amplitude weights are equal and normalized among those which go to the same dots. The phase of probability amplitudes are π when edges have weight -1 , and 0 otherwise.

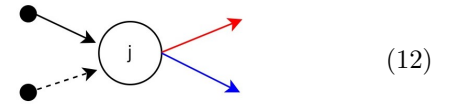
find schemes for genuinely entangled states, which are enumerated in Fig. 1. To design counterparts in linear optical circuits to the EPM bigraphs that generate the same entangled states, we need to know how each element of the graphs is translated to linear optical operators. A prerequisite for the translation rules from graphs to circuits is to provide heralded linear optical operators (which we name *subtractors*) that play the role of subtraction operators, because they are the fundamental components of EPM sculpting bigraphs. Appendix A explains how we can obtain such subtractors in linear optical networks. In this section, with the results in Appendix A as building blocks, we enumerate all the elements that construct EPM directed bigraphs and present translation rules of them to linear optical elements.

A. Translation rules

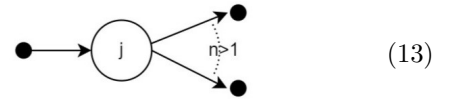
An arbitrary EPM directed bigraph that corresponds to a sculpting operator of a $(N + K)$ -partite system (N spatial modes in the main system and K spatial modes in the ancillary system) consists of the following elements:

1. N circles (labelled vertices) to which edges are

attached as



2. K circles to which edges are attached as



3. Dots (unlabelled vertices) with q incoming edges from the N circles of the form (12) and k incoming edges from the K circles of the form (13):



where the gray color of edges denotes that the edges can have any color between red and blue.

Among this elements, the following form

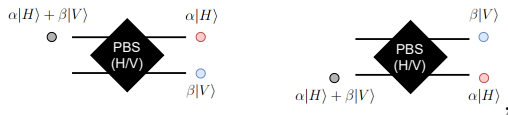


can be treated distinctly as it corresponds to an *optimized subtractor* (see Appendix A for the meaning of the optimized subtractor and why the above component can correspond to an optima subtractor).

The EPM sculpting bigraphs that generate essential multipartite entangled states are given in Fig. 1. We can check that $K = 0$ for the GHZ graph, $K = 1$ for the W graph, and $K = 3$ for $N = 3$ arbitrary entanglement graph.

We can impose translation rules of elements in EPM directed bigraphs to optical components. While a detailed explanation on the relations between two sides are given in Appendix A, we enumerate here the translation rules that we need for building circuits based on the graphs in Fig. 1.

In our setup, the internal boson states $\{|0\rangle, |1\rangle, |+\rangle, |-\rangle\}$ are encoded as the polarization of photons $\{|D\rangle, |A\rangle, |H\rangle, |V\rangle\}$ where (D =diagonal, A =antidiagonal, H = horizontal, V =vertical). And all the linear optical operators that we need are polarizing beam splitters (PBSs) that transform photons as

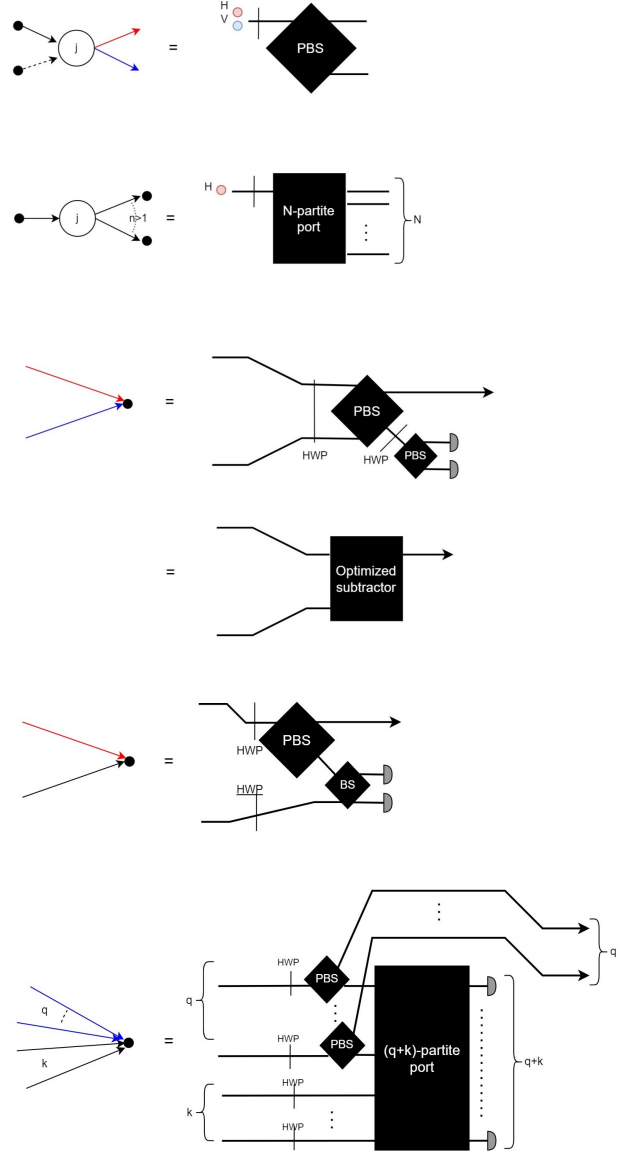


half-wave plates (HWPs) with

- HWP: $\{H, V\} \leftrightarrow \{D, A\}$
- $\underline{\text{HWP}}$: $\{H, V\} \leftrightarrow \{A, D\}$,

and K -partite multiports that Fourier-transform the spatial mode states of photons.

Translation rules



In the last equality of the above rules, if the edge from the j th circle is red (blue), the corresponding wire is attached to the upper (lower) mode of the j th PBS. And the q open wires go back to the spatial modes from which those wires came and be merged by PBSs.

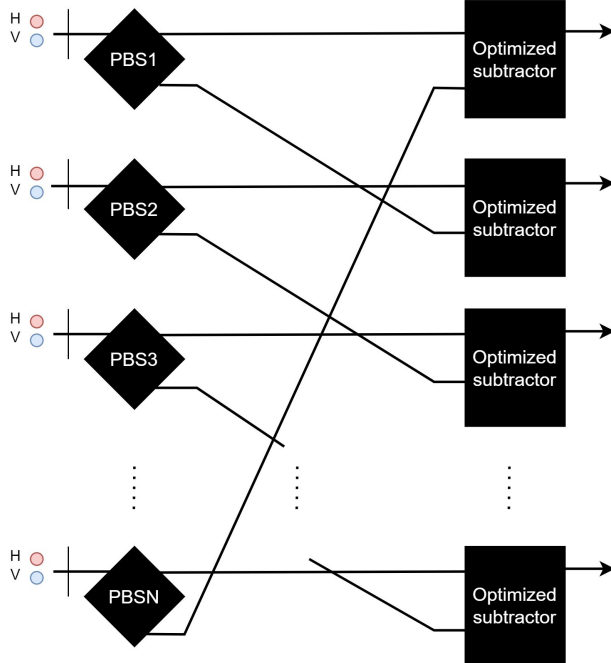
We can apply the above translation rules to any sculpting directed bigraphs including the N -partite GHZ, N -partite W, and $N = 3$ Type 5 state in Fig. 1.

B. N -partite GHZ state (Fig. 1 (a))

The GHZ generating EPM bigraph (Fig. 1 (a)) leads to the following operational form

$$\begin{aligned} \hat{A}_N |Sym_N\rangle &= \frac{1}{\sqrt{2^N}} \prod_{j=1}^N (\hat{a}_{j,+} + \hat{a}_{j\oplus N1,-}) |vac\rangle \\ &= \frac{1}{\sqrt{2^N}} \left(\prod_{j=1}^N \hat{a}_{j,+}^\dagger + (-1)^N \prod_{j=1}^N \hat{a}_{j,-}^\dagger \right) |vac\rangle. \end{aligned} \quad (16)$$

Following the translation rules, we have a simple linear optical circuit for the GHZ state as



Considering each optimized operator as a dot, we can see that the wires are connected following the structure of the GHZ sculpting bigraph.

The explicit calculation for showing that the above circuit generates the GHZ state is given in Appendix B. The success probability P_{suc} is $\frac{1}{2^{2N-1}}$ with feed-forward.

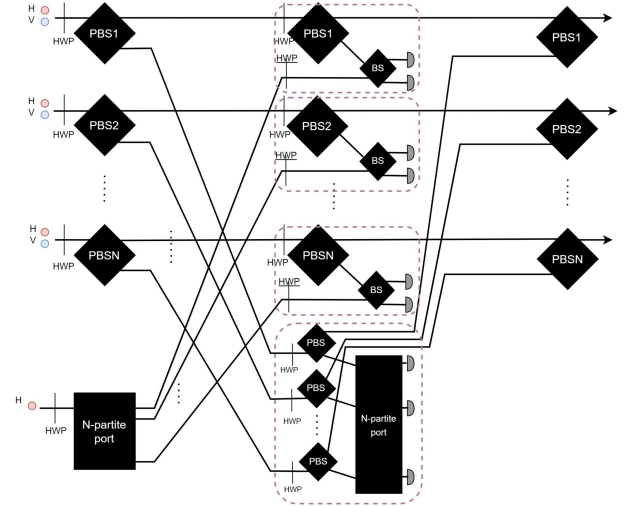
We can compare the above circuit with other heralded schemes for generating the GHZ state. Unlike Ref. [18] that suggests schemes for $N = 2$ and 3 , our scheme can be straightforwardly generalized to any N -partite case. There also exists a scheme for N -partite GHZ state with dual-rail encoding [19], however P_{suc} ($= \frac{1}{2^{3N-3}}$) in it is much lower than ours.

C. N -partite W state (Fig. 1, (b))

The W generating EPM bigraph (Fig. 1, (b)) leads to the following operational form

$$\begin{aligned} \hat{A}_{N+1} |Sym_N\rangle |Anc_1\rangle &= \frac{1}{\sqrt{2^N N}} \left(\prod_{j=1}^N (\hat{a}_{j,+} + \hat{a}_{X0}) \right) \sum_{k=1}^N \hat{a}_{k,-} \\ &\times \left(\prod_{m=1}^N \hat{a}_{m0}^\dagger \hat{a}_{m1}^\dagger \right) \hat{a}_{X0}^\dagger |vac\rangle \\ &= \frac{1}{\sqrt{2^N N}} (\hat{a}_{1,-}^\dagger \hat{a}_{2,+}^\dagger \cdots \hat{a}_{N+}^\dagger + \hat{a}_{1,+}^\dagger \hat{a}_{2,-}^\dagger \cdots \hat{a}_{N+}^\dagger \\ &\quad + \cdots + \hat{a}_{1,+}^\dagger \hat{a}_{2,+}^\dagger \cdots \hat{a}_{N-}^\dagger) |vac\rangle. \end{aligned} \quad (17)$$

A linear optical scheme for the above graph from the translation rules become the following circuit:



Considering each dashed purple box (spatially overlapped subtractors) as a dot, we can see that the wires are connected following the structure of the W sculpting bigraph.

Appendix C provides the explicit calculation for showing that the above circuit generates the W state. $P_{suc} = \frac{1}{2^{2N}}$ with feed-forward. Since our scheme requires $2N + 1$ single-photon sources for the N -partite W state, it is more feasible than those schemes that exploit fusion gates and smaller size of W states as resources for generating N -partite W states [20, 21].

D. $N = 3$ Type 5 state (Fig. 1 (c))

In case of the $N = 3$ entanglement, the GHZ state and W state stand out as representative states of

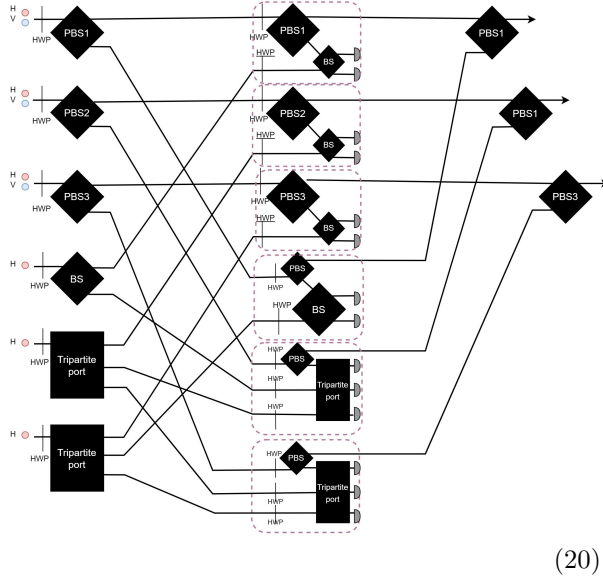
two distinct categories of genuine tripartite entanglement. Therefore, a superposed state of GHZ and W states can be a useful resource that cannot be generated by local operations and classical communications (LOCCs) to either GHZ or W states. We can express such states as a superposition of five local bases product states $\{|000\rangle, |100\rangle, |110\rangle, |101\rangle, |111\rangle\}$ ($N = 3$ Type 5 state [16]), which are locally equivalent to

$$\{|+++\rangle, |-++\rangle, |--+\rangle, |+-+\rangle, |---\rangle\}. \quad (18)$$

We can obtain such a state with the $N = 3$ Type-5 state generating EPM bigraph (Fig. 1 (c)), whose operational form is expressed as

$$\begin{aligned} & \hat{A}_{3+3}|Sym_3\rangle|Anc_3\rangle \\ &= \frac{1}{12}(\hat{a}_{1+} + \hat{a}_{X0})(\hat{a}_{2+} + \hat{a}_{Y0})(\hat{a}_{3+} + \hat{a}_{Z0}) \\ & \quad \times (\hat{a}_{Z0} - \hat{a}_{1-})(\hat{a}_{X0} + \hat{a}_{Y0} - \hat{a}_{2-})(\hat{a}_{Y0} + \hat{a}_{Z0} - \hat{a}_{3-}) \\ & \quad \times \left(\prod_{m=1}^3 \hat{a}_{m0}^\dagger \hat{a}_{m1}^\dagger \right) \hat{a}_{X0}^\dagger \hat{a}_{Y0}^\dagger \hat{a}_{Z0}^\dagger |vac\rangle \\ &= \frac{1}{12}(\hat{a}_{1+}^\dagger \hat{a}_{2+}^\dagger \hat{a}_{3+}^\dagger + \hat{a}_{1-}^\dagger \hat{a}_{2+}^\dagger \hat{a}_{3+}^\dagger + \hat{a}_{1-}^\dagger \hat{a}_{2+}^\dagger \hat{a}_{3-}^\dagger \\ & \quad + \hat{a}_{1-}^\dagger \hat{a}_{2-}^\dagger \hat{a}_{3+}^\dagger + \hat{a}_{1-}^\dagger \hat{a}_{2-}^\dagger \hat{a}_{3-}^\dagger) |vac\rangle \\ & \sim |+++\rangle + |-++\rangle + |--+\rangle + |+-+\rangle + |---\rangle. \end{aligned} \quad (19)$$

The corresponding optical circuit is



Considering each optimized operator as a dot, we can see that the wires are connected following the structure of the $N = 3$ Type 5 entangled state sculpting bigraph. See Appendix D for the explicit

calculation that generates $N = 3$ Type 5 entangled state with the above circuit. $P_{suc} = 5/(3^2 2^7)$ with feed-forward. To our knowledge, no heralded scheme has been proposed to generate $N = 3$ Type 5 state.

IV. DISCUSSIONS

By establishing a set of translation rules from sculpting bigraphs into linear optical circuits, we have proposed a systematic method to design heralded circuits for the multipartite entanglement of bosons. Although our work primarily addresses optical circuits employing polarization encoding, it is worth noting that conceptually equivalent circuits in dual-rail encoding can be readily considered.

The methodology discussed herein is applicable to any entanglement generating sculpting protocols using EPM sculpting bigraphs. For instance, Ref. [22] proposed a set of EPM sculpting bigraphs that generate a special type of graph states, i.e., caterpillar graph states. Our translation rules can be directly applied to the construction of heralded linear optical circuits for caterpillar graph states using the associated sculpting bigraphs. This implies that *we have successfully simplified the task of finding heralded schemes for generating entanglement into that of finding EPM bigraphs that correspond to suitable sculpting operators.*

We can extend our discussion to qudit entanglement generation, e.g., qudit N -partite GHZ states that we can also generate with the sculpting protocol as shown in Ref. [14], Sec. V. We can choose any photonic degree of freedom as the internal state for encoding qudits, e.g., orbital angular momentums (OAMs). Then the PBSs are replaced with OAM beam splitters [23] and HWPs with OAM-only Fourier transformation operators [24].

Additionally, we anticipate that our proposed schemes will be validated through real optical experiments in the near future. Alternatively, one can also use online quantum computing platforms such as Quandella [25] that offer the linear operations involving ideal photons by adopting our circuits into dual-rail encoding circuits.

ACKNOWLEDGEMENTS

SC is grateful to Prof. Ana Belen Sainz and Prof. Jung-Hoon Chun for their support on this research. This research is funded by National Research

Foundation of Korea (NRF, RS-2023-00245747, 2021M3H3A103657313, 2022M3K4A1094774, and 2023M3K5A1094805), Korea Institute of Science and Technology (2E31021), and Foundation for Polish Science (IRAP project, ICTQT, contract no.2018/MAB/5, co-financed by EU within Smart Growth Operational Programme)

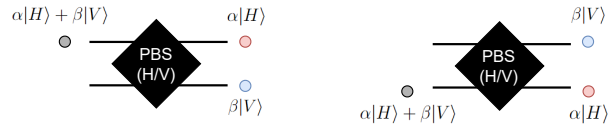
-
- [1] Martin B Plenio and Shashank Virmani. An introduction to entanglement measures. *Quantum Inf. Comput.*, 7(1):1–51, 2007.
- [2] John Preskill. Quantum computing and the entanglement frontier. *arXiv preprint arXiv:1203.5813*, 2012.
- [3] Nicolas Gisin, Grégoire Ribordy, Wolfgang Tittel, and Hugo Zbinden. Quantum cryptography. *Reviews of modern physics*, 74(1):145, 2002.
- [4] Charles H Bennett, Gilles Brassard, Claude Crépeau, Richard Jozsa, Asher Peres, and William K Wootters. Teleporting an unknown quantum state via dual classical and einstein-podolsky-rosen channels. *Physical Review Letters*, 70(13):1895, 1993.
- [5] Pankaj Agrawal and Arun Pati. Perfect teleportation and superdense coding with W states. *Physical Review A*, 74(6):062320, 2006.
- [6] Luca Pezze, Augusto Smerzi, Markus K Oberthaler, Roman Schmied, and Philipp Treutlein. Quantum metrology with nonclassical states of atomic ensembles. *Reviews of Modern Physics*, 90(3):035005, 2018.
- [7] Mariana R Barros, Seungbeom Chin, Tanumoy Pramanik, Hyang-Tag Lim, Young-Wook Cho, Joonsuk Huh, and Yong-Su Kim. Entangling bosons through particle indistinguishability and spatial overlap. *Optics Express*, 28(25):38083–38092, 2020.
- [8] Seungbeom Chin, Yong-Su Kim, and Sangmin Lee. Graph picture of linear quantum networks and entanglement. *Quantum*, 5:611, 2021.
- [9] Donghwa Lee, Tanumoy Pramanik, Seongjin Hong, Young-Wook Cho, Hyang-Tag Lim, Seungbeom Chin, and Yong-Su Kim. Entangling three identical particles via spatial overlap. *Optics Express*, 30(17):30525–30535, 2022.
- [10] Jeremy C Adcock, Sam Morley-Short, Joshua W Silverstone, and Mark G Thompson. Hard limits on the postselectability of optical graph states. *Quantum Science and Technology*, 4(1):015010, 2018.
- [11] Jonas Zeuner, Aditya N Sharma, Max Tillmann, René Heilmann, Markus Gräfe, Amir Moqanaki, Alexander Szameit, and Philip Walther. Integrated-optics heralded controlled-not gate for polarization-encoded qubits. *npj Quantum Information*, 4(1):13, 2018.
- [12] Jin-Peng Li, Xuemei Gu, Jian Qin, Dian Wu, Xiang You, Hui Wang, Christian Schneider, Sven Höfling, Yong-Heng Huo, Chao-Yang Lu, et al. Heralded nondestructive quantum entangling gate with single-photon sources. *Physical Review Letters*, 126(14):140501, 2021.
- [13] Dat Thanh Le, Warit Asavanant, and Nguyen Ba An. Heralded preparation of polarization entanglement via quantum scissors. *Physical Review A*, 104(1):012612, 2021.
- [14] Seungbeom Chin, Yong-Su Kim, and Marcin Karczewski. Graph approach to entanglement generation by boson subtractions. *arXiv preprint arXiv:2211.04042*, 2022.
- [15] Marcin Karczewski, Su-Yong Lee, Junghee Ryu, Zakarya Lasmar, Dagomir Kaszlikowski, and Paweł Kurzyński. Sculpting out quantum correlations with bosonic subtraction. *Physical Review A*, 100(3):033828, 2019.
- [16] Antonio Acín, A Andrianov, L Costa, E Jané, JI Latorre, and Rolf Tarrach. Generalized schmidt decomposition and classification of three-quantum-bit states. *Physical Review Letters*, 85(7):1560, 2000.
- [17] Michael Walter, David Gross, and Jens Eisert. Multipartite entanglement. *Quantum Information: From Foundations to Quantum Technology Applications*, pages 293–330, 2016.
- [18] FV Gubarev, IV Dyakonov, M Yu Saygin, GI Struchalin, SS Straupe, and SP Kulik. Improved heralded schemes to generate entangled states from single photons. *Physical Review A*, 102(1):012604, 2020.
- [19] XB Zou, K Pahlke, and W Mathis. Generation of a multi-photon greenberger–horne–zeilinger state with linear optical elements and photon detectors. *Journal of Optics B: Quantum and Semiclassical Optics*, 7(4):119, 2005.
- [20] Ş K Özdemir, Eiji Matsunaga, Toshiyuki Tashima, Takashi Yamamoto, Masato Koashi, and Nobuyuki Imoto. An optical fusion gate for W-states. *New Journal of Physics*, 13(10):103003, 2011.
- [21] Ke Li, Dongliang Zheng, Wangqiong Xu, Huibing Mao, and Jiqing Wang. W states fusion via polarization-dependent beam splitter. *Quantum Information Processing*, 19(11):412, 2020.
- [22] Seungbeom Chin. From linear quantum system graphs to qubit graphs: Heralded generation of graph states. *arXiv preprint arXiv:2306.15148*, 2023.
- [23] XuBo Zou and W Mathis. Scheme for optical implementation of orbital angular momentum beam splitter of a light beam and its application in quantum information processing. *Physical Review A*, 71(4):042324, 2005.

[24] Jaroslav Kysela, Xiaoqin Gao, and Borivoje Dakić. Fourier transform of the orbital angular momentum of a single photon. *Physical Review Applied*, 14(3):034036, 2020.

[25] Nicolas Maring, Andreas Fyrillas, Mathias Pont, Edouard Ivanov, Petr Stepanov, Nico Margaria, William Hease, Anton Pishchagin, Thi Huong Au, Sébastien Boissier, et al. A general-purpose single-photon-based quantum computing platform. *arXiv preprint arXiv:2306.00874*, 2023.

Appendix A: Subtraction operators with heralding

The essential part in a EPM directed bigraph is the right hand side of the graph from the circles as it represents the sculpting operator that generates entanglement. To design associated optical circuits from the EPM sculpting bigraphs, we need to define heralded operators for subtracting single bosons, which we name *subtractors*. In this section, We will show that such operators can be constructed in linear optics with compositions of following operators: polarizing beam splitters (PBSs) that transform photons as



half-wave plates (HWPs) with

- HWP: $\{H, V\} \leftrightarrow \{D, A\}$
- HWP: $\{H, V\} \leftrightarrow \{A, D\}$,

and K -partite multiports that Fourier-transform the spatial mode states of photons. This also implies that any bosonic system that has linear operators with the same effect can generate entanglement with our schemes.

We start from the heralded schemes for the identities (7), whose operational expressions become

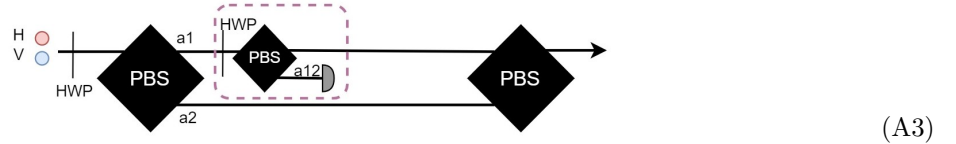
$$\hat{a}_{\pm} \hat{a}_0^{\dagger} \hat{a}_1^{\dagger} |vac\rangle = \pm \hat{a}_{\pm}^{\dagger} |vac\rangle \quad (\text{A1})$$

as this is a fundamental element for EPM directed bigraphs.

We first consider the heralded optical circuit for taking \hat{a}_+ , which can be rewritten as

$$\hat{a}_+ \frac{(\hat{a}_+^{\dagger 2} - \hat{a}_-^{\dagger 2})}{2} |vac\rangle = \hat{a}_+^{\dagger} |vac\rangle. \quad (\text{A2})$$

This operation is implemented with a linear optical scheme as



by encoding the internal degree of freedom with the photon polarization as

$$\{|0\rangle, |1\rangle\} \cong \{|D\rangle, |A\rangle\}, \quad \{|+\rangle, |-\rangle\} \cong \{|H\rangle, |V\rangle\}. \quad (\text{A4})$$

Step-by-step explanation

1. The 1st HWP: Preparation of the initial state

$$\hat{a}_H^{\dagger} \hat{a}_V^{\dagger} \rightarrow \hat{a}_D^{\dagger} \hat{a}_A^{\dagger} = \frac{1}{2} (\hat{a}_H^{\dagger 2} - \hat{a}_A^{\dagger 2}) \quad (\text{A5})$$

2. The 1st PBS: Division of the particles with different internal states into two distinguishable spatial modes:

$$\frac{1}{2}(\hat{a}_H^{\dagger 2} - \hat{a}_V^{\dagger 2}) \rightarrow \frac{1}{2}(\hat{a}_{1,H}^{\dagger 2} - \hat{a}_{2,V}^{\dagger 2}) \quad (\text{A6})$$

where 1 and 2 denote the upper and lower paths of PBS respectively.

3. The dashed purple box: Subtraction of $\hat{a}_{1,H}^{\dagger}$ by a measurement in which exactly one photon is registered in mode 12

$$\frac{1}{2}(\hat{a}_{1,H}^{\dagger 2} - \hat{a}_{2,V}^{\dagger 2}) \rightarrow \hat{a}_{1,H}^{\dagger} \quad (\text{A7})$$

We can see that the measurement of one photon at the detector 12 corresponds to the subtraction of one photon.

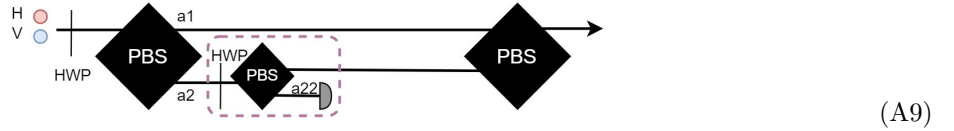
4. The last PBS: Mergence of the particle paths by which the photon always arrives at one spatial mode:

$$\hat{a}_{1H}^{\dagger} \rightarrow \hat{a}_H^{\dagger} \quad (\text{A8})$$

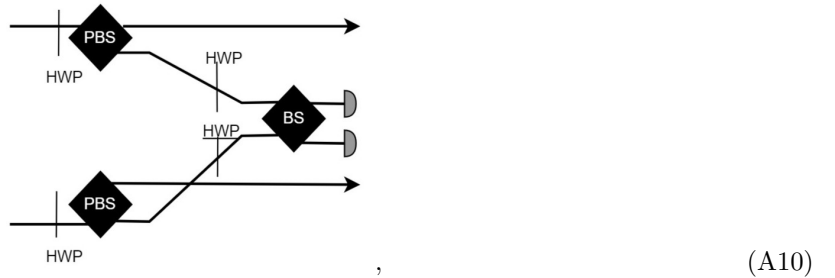
Note that the dashed purple box corresponds to a particle subtraction by postselection, which we name a *subtractor*.

In the above process, we can obtain the same result by simply attenuating the lower wire instead of merging two paths of wires by the last PBS, which however is needed for the general cases when the heralded subtraction is overlapped among several spatial modes.

The circuit for taking \hat{a}_- can be designed similarly as



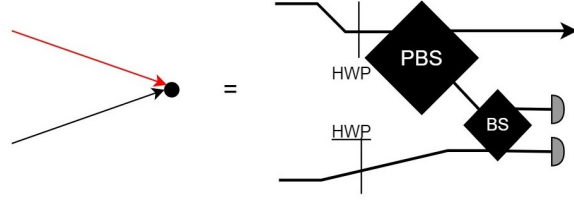
We can generalize the above subtractor to spatially overlapped subtractions (i.e., a single-boson subtraction operator $\hat{A}^{(l)}$ is a superposition of subtractions on different spatial modes) from k different spatial modes by superposing the paths of detected particles. Hence, for example, a subtraction ($\hat{a}_{1+} - \hat{a}_{2-}$) from two modes 1 and 2 corresponds to



where the incoming wires are attached to 11 and 22 by the internal states of the annihilation operators. In the above subtractor, the two open wires go back to the spatial modes from which those wires came and be merged by PBSs as in (A3) and (A9).

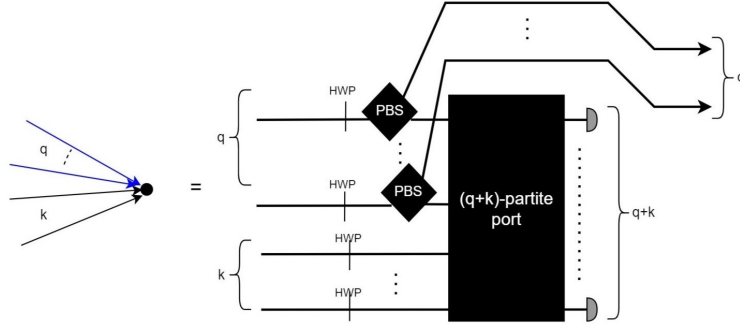
In the most general sense, we can subtract a photon from more than l (≥ 2) modes, some from the main system (two photons per mode) and some from the ancillary system (one photon per mode). For the case, we place a PBS on the path from the main system and make a measurement in the mutually unbiased basis using K -partite port. Based on this principle, we can build the subtractors needed for the EPM sculpting

bigraphs in our work:



(A11)

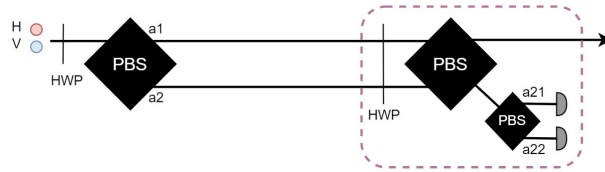
and



(A12)

where we postselect the case when only one photon arrives at the detectors of the above two subtractors. In the subtractor (A12), the q open wires go back to the spatial modes from which those wires came and are merged by PBSs as in (A3) and (A9).

On the other hand, we can also provide an alternative circuit that plays the roles of circuits (A3) and (A9) simultaneously:



(A13)

The dashed purple box of the above circuit becomes a subtraction operator with heralding, for we can subtract \hat{a}_+ (\hat{a}_-) by postselecting the outputs when a particle arrives at the lower (upper) mode of the last PBS.

Step-by-step explanation

1. The 1st HWP: Preparation of the initial state

$$\hat{a}_H^\dagger \hat{a}_V^\dagger \rightarrow \hat{a}_D^\dagger \hat{a}_A^\dagger = \frac{1}{2}(\hat{a}_H^{\dagger 2} - \hat{a}_A^{\dagger 2}) \quad (\text{A14})$$

2. The 1st PBS: Division of the photon paths following the internal states:

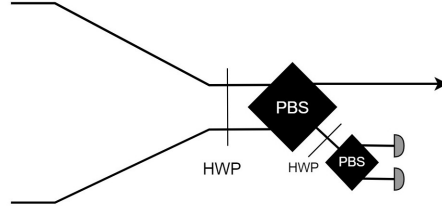
$$\frac{1}{2}(\hat{a}_H^{\dagger 2} - \hat{a}_V^{\dagger 2}) \rightarrow \frac{1}{2}(\hat{a}_{1,H}^{\dagger 2} - \hat{a}_{2,V}^{\dagger 2}) \quad (\text{A15})$$

3. The dashed purple box: Subtraction of $\hat{a}_{1,H}^\dagger$ or $\hat{a}_{2,V}^\dagger$ by heralding

$$\begin{aligned} \frac{1}{2}(\hat{a}_{1,H}^{\dagger 2} - \hat{a}_{2,V}^{\dagger 2}) &\xrightarrow{HWP} \frac{1}{2}(\hat{a}_{1,D}^{\dagger 2} - \hat{a}_{2,A}^{\dagger 2}) \\ &\xrightarrow{PBS} \frac{1}{4} \left((\hat{a}_{1,H}^\dagger + \hat{a}_{2,V}^\dagger)^2 - (\hat{a}_{2,H}^\dagger - \hat{a}_{1,V}^\dagger)^2 \right) \\ &\xrightarrow{P.S.} \hat{a}_{1,H}^\dagger \hat{a}_{22,V}^\dagger \text{ or } \hat{a}_{1,V}^\dagger \hat{a}_{21,H}^\dagger \end{aligned} \quad (\text{A16})$$

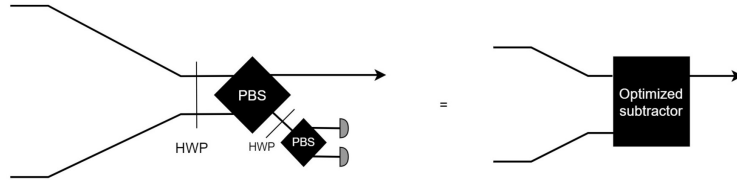
The postselection of one-photon state corresponds to a photon subtraction. A photon with V in the upper mode (H in the lower mode) heralds \hat{a}_H^\dagger (\hat{a}_V^\dagger).

We can use this alternative subtraction operator when the one-boson subtraction operator is a superposition of two annihilation operators and their internal state is orthogonal to each other. $(\hat{a}_+ - \hat{b}_-)$ is an example of such an operator. Then,



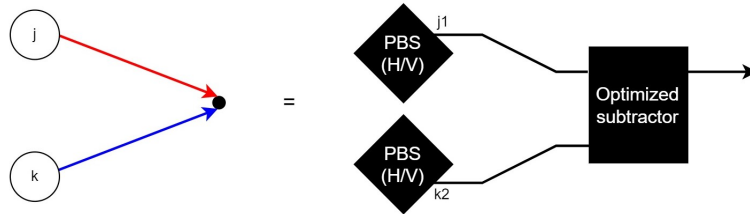
(A17)

subtracts one photon in a spatially overlapped way when a photon arrives at either upper or lower detector. In the above operator, we need an HWP between two PBSs, with which we can generate the spatially overlapped subtractor of different internal states from difference input modes. We define the above operator as an *optimized subtractor* as it needs less PBSs than the subtractor (A10), denoting it as



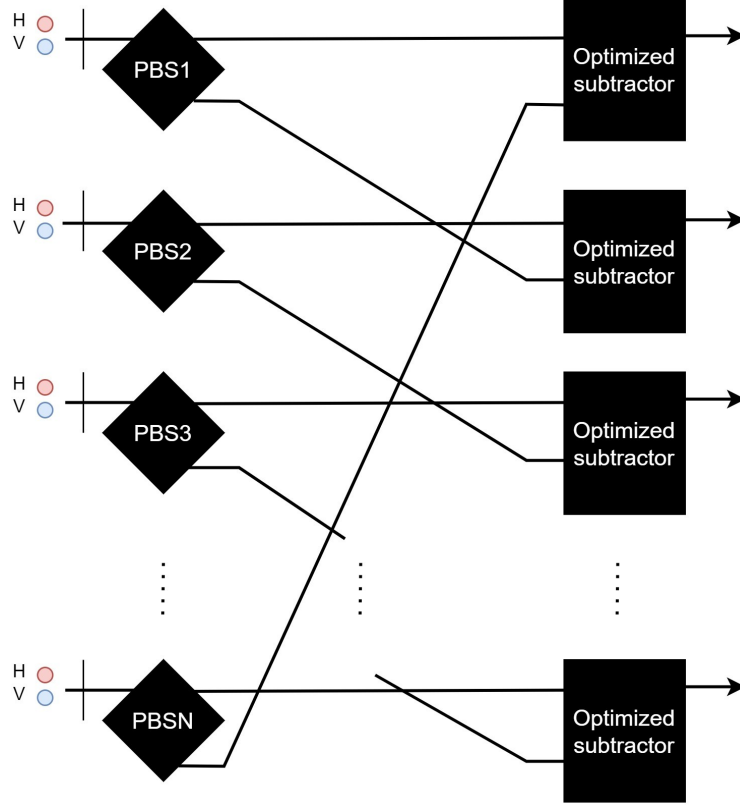
(A18)

In the graph picture, we obtain the following equality:



(A19)

Appendix B: GHZ state



Here spatial modes are denoted as $\{1, 2, \dots, N\}$.

- Step 1. Preparation of the initial state

$$\prod_{j=1}^N \hat{a}_{j,H}^\dagger \hat{a}_{j,V}^\dagger \rightarrow \prod_{j=1}^N \hat{a}_{j,D}^\dagger \hat{a}_{j,A}^\dagger \quad (\text{B1})$$

- Step 2. Divide the photon paths according to the polarization

$$\prod_{j=1}^N \hat{a}_{j,D}^\dagger \hat{a}_{j,A}^\dagger \rightarrow \frac{1}{2^N} \prod_{j=1}^N (\hat{a}_{j1,H}^{\dagger 2} - \hat{a}_{j2,V}^{\dagger 2}) \quad (\text{B2})$$

- Step 3. Swapping among wires

$$\frac{1}{2^N} \prod_{j=1}^N (\hat{a}_{j1,H}^{\dagger 2} - \hat{a}_{j2,V}^{\dagger 2}) \rightarrow \frac{1}{2^N} \prod_{j=1}^N (\hat{a}_{j1,H}^{\dagger 2} - \hat{a}_{(j \oplus_N)2,V}^{\dagger 2}) \quad (\text{B3})$$

where \oplus_N is an addition modulo N .

- Step 4. Subtractions are performed in two steps. First, the state is transformed by HWP and PBSs in

the optimized subtractors as

$$\begin{aligned}
& \frac{1}{2^N} \prod_{j=1}^N (\hat{a}_{j1,H}^{\dagger 2} - \hat{a}_{(j\oplus N)2,V}^{\dagger 2}) \rightarrow \\
& \frac{1}{2^{2N}} \prod_{j=1}^N \left((\hat{a}_{j1,H}^{\dagger} + \hat{a}_{j2,V}^{\dagger})^2 - (\hat{a}_{(j\oplus N)2,H}^{\dagger} - \hat{a}_{(j\oplus N)1,V}^{\dagger})^2 \right) \\
& = \frac{1}{2^{2N}} \prod_{j=1}^N \left((\hat{a}_{j1,H}^{\dagger 2} + 2\hat{a}_{j1,H}^{\dagger} \hat{a}_{j2,V}^{\dagger} + \hat{a}_{j2,V}^{\dagger 2}) - (\hat{a}_{(j\oplus N)2,H}^{\dagger 2} + 2\hat{a}_{(j\oplus N)2,H}^{\dagger} \hat{a}_{(j\oplus N)1,V}^{\dagger} + \hat{a}_{(j\oplus N)1,V}^{\dagger 2}) \right). \quad (\text{B4})
\end{aligned}$$

Then we postselections the states with exactly one photon between two detectors attached to the PBS in each optimized subtractor, hence the only states that contribute to the final state are

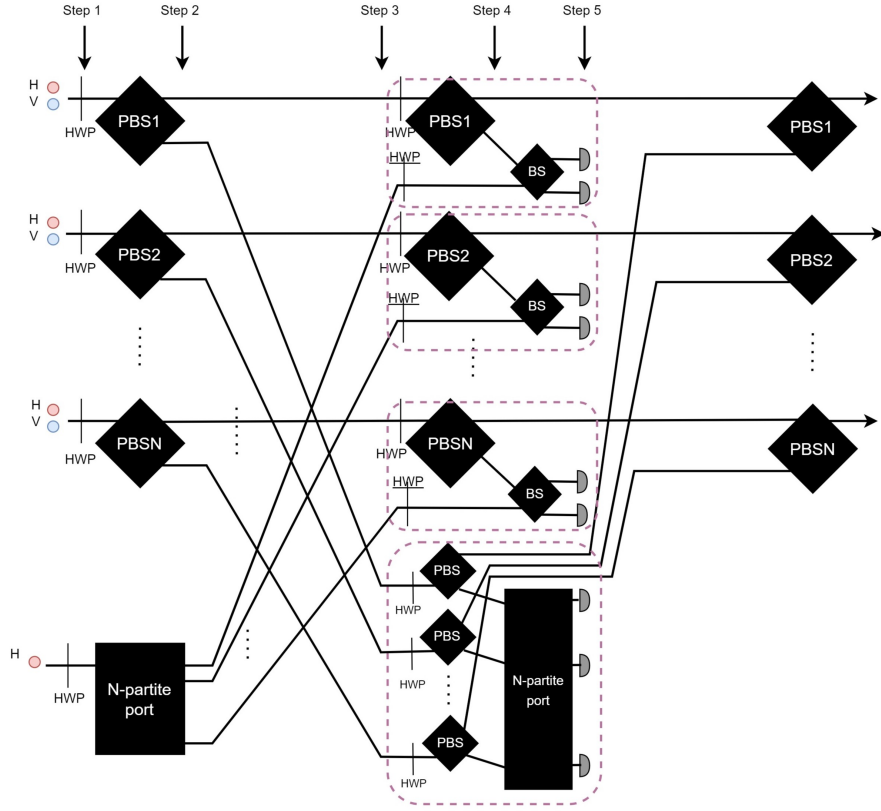
$$\frac{1}{2^{N-\frac{1}{2}}} \frac{\left(\prod_{j=1}^N (\hat{a}_{j1,H}^{\dagger} \hat{a}_{j2,V}^{\dagger}) + (-1)^N \prod_{j=1}^N (\hat{a}_{(j\oplus N)2,H}^{\dagger} \hat{a}_{(j\oplus N)1,V}^{\dagger}) \right)}{\sqrt{2}}, \quad (\text{B5})$$

which becomes an N -partite GHZ state after the measurements in the optimized subtractors. For example, when all the heralding particles are detected at the upper mode of the PBSs in the optimized subtractors, the state becomes

$$\begin{aligned}
& \frac{1}{\sqrt{2}} \left(\prod_{j=1}^N \hat{a}_{j1,H}^{\dagger} + (-1)^N \prod_{j=1}^N \hat{a}_{(j\oplus N)1,V}^{\dagger} \right) |vac\rangle \\
& = \frac{1}{\sqrt{2}} \left(\prod_{j=1}^N \hat{a}_{j1,H}^{\dagger} + (-1)^N \prod_{j=1}^N \hat{a}_{j1,V}^{\dagger} \right) |vac\rangle. \quad (\text{B6})
\end{aligned}$$

The success probability is $\frac{1}{2^{2N}}$ without feed-forward, which becomes $\frac{1}{2^{2N-1}}$ with feed-forward.

Appendix C: W state



Even if the above circuit is obtained directly from the translation rules from EPM bigraphs to circuits, we can obtain the same final state with fewer operators by changing the initial polarization of the photon in the ancillary mode to V instead of H and removing the HWP before the N -partite port and HWPs in the subtractors. Spatial modes are denoted as $\{1, 2, \dots, N, X\}$.

- Step 1. Preparation of the initial state

$$\left(\prod_{j=1}^N \hat{a}_{j,H}^\dagger \hat{a}_{j,V}^\dagger \right) \hat{a}_{X,H}^\dagger \rightarrow \left(\prod_{j=1}^N \hat{a}_{j,D}^\dagger \hat{a}_{j,A}^\dagger \right) \hat{a}_{X,D}^\dagger \quad (\text{C1})$$

- Step 2. Division of the photon paths with N PBSs and one N -partite port

$$\left(\prod_{j=1}^N \hat{a}_{j,D}^\dagger \hat{a}_{j,A}^\dagger \right) \hat{a}_{X,D}^\dagger \rightarrow \frac{1}{2^N \sqrt{N}} \prod_{j=1}^N (\hat{a}_{j1,H}^{\dagger 2} - \hat{a}_{j2,V}^{\dagger 2}) \sum_{k=1}^N \hat{a}_{Xk,D}^\dagger \quad (\text{C2})$$

- Step 3. Permutation of wires

$$\frac{1}{2^N \sqrt{N}} \prod_{j=1}^N (\hat{a}_{j1,H}^{\dagger 2} - \hat{a}_{j2,V}^{\dagger 2}) \sum_{k=1}^N \hat{a}_{Xk,D}^\dagger \rightarrow \frac{1}{2^N \sqrt{N}} \prod_{j=1}^N (\hat{a}_{j1,H}^{\dagger 2} - \hat{a}_{Xj,V}^{\dagger 2}) \sum_{k=1}^N \hat{a}_{k3,D}^\dagger \quad (\text{C3})$$

where we denote $k3$ ($k \in \{1, 2, \dots, N\}$) as the paths from the ancillary N -partite port to each detector of the main system.

- Step 4. Splitting two-photon states with HWPs and PBSs

$$\begin{aligned}
& \frac{1}{2^N \sqrt{N}} \prod_{j=1}^N (\hat{a}_{j1,H}^{\dagger 2} - \hat{a}_{Xj,V}^{\dagger 2}) \sum_{k=1}^N \hat{a}_{k3,D}^{\dagger} \\
& \rightarrow \frac{1}{2^N \sqrt{N}} \prod_{j=1}^N (\hat{a}_{j1,D}^{\dagger 2} - \hat{a}_{Xj,A}^{\dagger 2}) \sum_{k=1}^N \hat{a}_{k3,V}^{\dagger} \\
& \rightarrow \frac{1}{2^{2N} \sqrt{N}} \prod_{j=1}^N \left((\hat{a}_{j1,H}^{\dagger} + \hat{a}_{j2,V}^{\dagger})^2 - (\hat{a}_{Xj2,H}^{\dagger} - \hat{a}_{Xj1,V}^{\dagger})^2 \right) \sum_{k=1}^N \hat{a}_{k3,V}^{\dagger} \\
& = \frac{1}{2^{2N} \sqrt{N}} \prod_{j=1}^N \left((\hat{a}_{j1,H}^{\dagger 2} + 2\hat{a}_{j1,H}^{\dagger} \hat{a}_{j2,V}^{\dagger} + \hat{a}_{j2,V}^{\dagger 2}) - (\hat{a}_{Xj2,H}^{\dagger 2} - 2\hat{a}_{Xj2,H}^{\dagger} \hat{a}_{Xj1,V}^{\dagger} + \hat{a}_{Xj1,V}^{\dagger 2}) \right) \sum_{k=1}^N \hat{a}_{k3,V}^{\dagger} \quad (C4)
\end{aligned}$$

- Step 5. Postselection of states with one photon among the detectors attached to the last set of PBSs and N -partite port, by which the states that contribute to the final state are

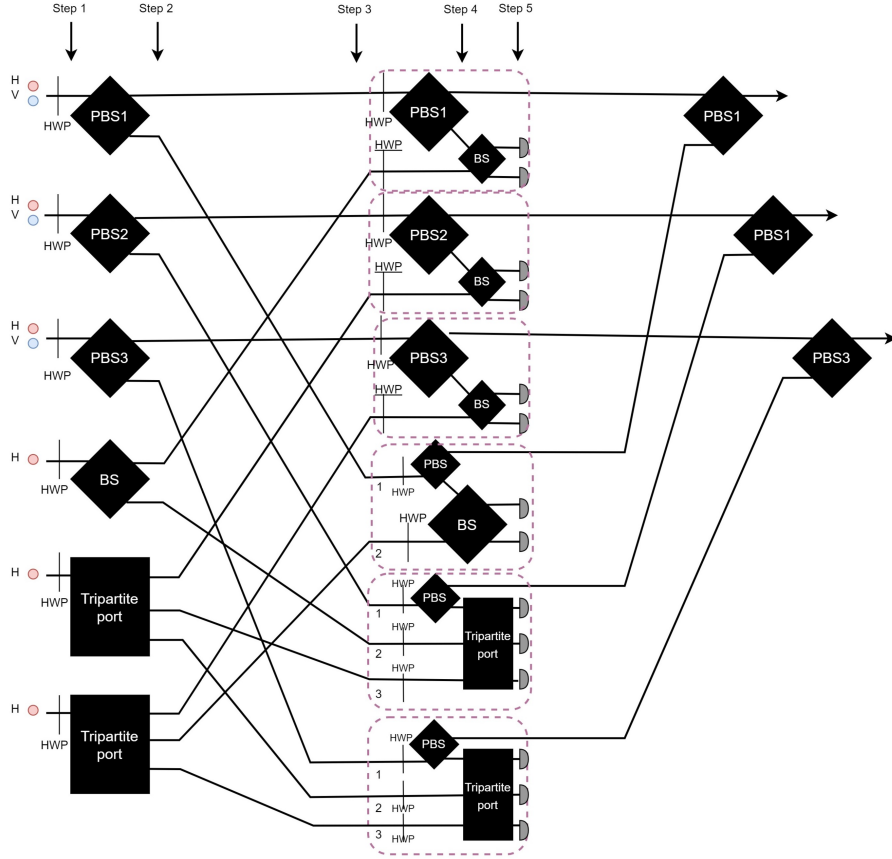
$$\frac{1}{2^N \sqrt{N}} \sum_{k=1}^N \left(\hat{a}_{k2,V}^{\dagger} \hat{a}_{Xk2,D}^{\dagger} \hat{a}_{k,V}^{\dagger} \prod_{j \neq k}^N \hat{a}_{j,H}^{\dagger} \hat{a}_{j2,V}^{\dagger} \right) \quad (C5)$$

which becomes the N -partite W state with heralding. For example, if all the photons are detected in the upper-most mode in each subtractor, the state becomes

$$\frac{1}{\sqrt{N}} \sum_{k=1}^N \left(\hat{a}_{k,V}^{\dagger} \prod_{j \neq k}^N \hat{a}_{j,H}^{\dagger} \right) |vac\rangle. \quad (C6)$$

The success probability is $\frac{1}{N 2^{2N+1}}$ without feed-forward, which becomes $\frac{1}{2^{2N}}$ with feed-forward.

Appendix D: $N = 3$ Type 5 entangled state



(D1)

Here spatial modes are denoted as $\{1, 2, 3, X, Y, Z\}$.

- Step 1. Preparation of the initial state

$$\left(\prod_{j=1}^3 \hat{a}_{j,H}^\dagger \hat{a}_{j,V}^\dagger \right) \hat{a}_{X,H}^\dagger \hat{a}_{Y,H}^\dagger \hat{a}_{Z,H}^\dagger \rightarrow \left(\prod_{j=1}^N \hat{a}_{j,D}^\dagger \hat{a}_{j,A}^\dagger \right) \hat{a}_{X,D}^\dagger \hat{a}_{Y,D}^\dagger \hat{a}_{Z,D}^\dagger \quad (D2)$$

- Step 2. Division of the photon paths with three PBSs, one BS, and two tripartite ports (tritters)

$$\left(\prod_{j=1}^N \hat{a}_{j,D}^\dagger \hat{a}_{j,A}^\dagger \right) \hat{a}_{X,D}^\dagger \hat{a}_{Y,D}^\dagger \hat{a}_{Z,D}^\dagger \rightarrow \frac{1}{24\sqrt{2}} \prod_{j=1}^3 (\hat{a}_{j1,H}^{\dagger 2} - \hat{a}_{j2,V}^{\dagger 2}) (\hat{a}_{X1,D}^\dagger + \hat{a}_{X2,D}^\dagger) \sum_{k=1}^3 \hat{a}_{Yk,D}^\dagger \sum_{l=1}^3 \hat{a}_{Zl,D}^\dagger \quad (D3)$$

Here (X, Y, Z) has $(2,3,3)$ spatial modes respectively, which are labelled as in the three lower purple boxes.

- Step 3. Permutation of wires

$$\frac{1}{24\sqrt{2}} (\hat{a}_{11,H}^{\dagger 2} - \hat{a}_{X1,V}^{\dagger 2}) (\hat{a}_{21,H}^{\dagger 2} - \hat{a}_{Y1,V}^{\dagger 2}) (\hat{a}_{31,H}^{\dagger 2} - \hat{a}_{Z1,V}^{\dagger 2}) \times (\hat{a}_{13,D}^\dagger + \hat{a}_{Y2,D}^\dagger) (\hat{a}_{23,D}^\dagger + \hat{a}_{Y3,D}^\dagger + \hat{a}_{Z2,D}^\dagger) (\hat{a}_{33,D}^\dagger + \hat{a}_{X2,D}^\dagger + \hat{a}_{Z3,D}^\dagger) \quad (D4)$$

where we denote $k3$ ($k \in \{1, 2, 3\}$) as the paths from the ancillary modes to each detector of the main system.

- Step 4. Splitting two-photon states with HWPs and PBSs

$$\begin{aligned}
& \frac{1}{24\sqrt{2}} \left(\hat{a}_{11,D}^{\dagger 2} - \hat{a}_{X1,A}^{\dagger 2} \right) \left(\hat{a}_{21,D}^{\dagger 2} - \hat{a}_{Y1,A}^{\dagger 2} \right) \left(\hat{a}_{31,D}^{\dagger 2} - \hat{a}_{Z1,A}^{\dagger 2} \right) \\
& \quad \times \left(\hat{a}_{13,V}^{\dagger} + \hat{a}_{Y2,H}^{\dagger} \right) \left(\hat{a}_{23,V}^{\dagger} + \hat{a}_{Y3,H}^{\dagger} + \hat{a}_{Z2,H}^{\dagger} \right) \left(\hat{a}_{33,V}^{\dagger} + \hat{a}_{X2,H}^{\dagger} + \hat{a}_{Z3,H}^{\dagger} \right) \\
\rightarrow & \frac{1}{192\sqrt{2}} \left(\left(\hat{a}_{11,H}^{\dagger} + \hat{a}_{12,V}^{\dagger} \right)^2 - \left(\hat{a}_{X1,H}^{\dagger} - \hat{a}_{1,V}^{\dagger} \right)^2 \right) \left(\left(\hat{a}_{21,H}^{\dagger} + \hat{a}_{22,V}^{\dagger} \right)^2 - \left(\hat{a}_{Y1,H}^{\dagger} - \hat{a}_{2,V}^{\dagger} \right)^2 \right) \\
& \quad \times \left(\left(\hat{a}_{31,H}^{\dagger} + \hat{a}_{32,V}^{\dagger} \right)^2 - \left(\hat{a}_{Z1,H}^{\dagger} - \hat{a}_{3,V}^{\dagger} \right)^2 \right) \left(\hat{a}_{13,V}^{\dagger} + \hat{a}_{Y2,H}^{\dagger} \right) \left(\hat{a}_{23,V}^{\dagger} + \hat{a}_{Y3,H}^{\dagger} + \hat{a}_{Z2,H}^{\dagger} \right) \left(\hat{a}_{33,V}^{\dagger} + \hat{a}_{X2,H}^{\dagger} + \hat{a}_{Z3,H}^{\dagger} \right)
\end{aligned} \tag{D5}$$

- Step 5. Postselection on states with exactly one photon in the sets of detectors belonging to each of the subtractors, hence the states that contribute to the final states are

$$\begin{aligned}
& \frac{1}{24\sqrt{2}} \left(\hat{a}_{11,H}^{\dagger} \hat{a}_{12,V}^{\dagger} \hat{a}_{21,H}^{\dagger} \hat{a}_{22,V}^{\dagger} \hat{a}_{31,H}^{\dagger} \hat{a}_{32,V}^{\dagger} \hat{a}_{X2,H}^{\dagger} \hat{a}_{Y2,H}^{\dagger} \hat{a}_{Z3,H}^{\dagger} + \hat{a}_{X1,H}^{\dagger} \hat{a}_{1,V}^{\dagger} \hat{a}_{21,H}^{\dagger} \hat{a}_{22,V}^{\dagger} \hat{a}_{31,H}^{\dagger} \hat{a}_{32,V}^{\dagger} \hat{a}_{13,V}^{\dagger} \hat{a}_{Y2,H}^{\dagger} \hat{a}_{Z3,H}^{\dagger} \right. \\
& \quad + \hat{a}_{X1,H}^{\dagger} \hat{a}_{1,V}^{\dagger} \hat{a}_{21,H}^{\dagger} \hat{a}_{22,V}^{\dagger} \hat{a}_{Z1,H}^{\dagger} \hat{a}_{3,V}^{\dagger} \hat{a}_{13,V}^{\dagger} \hat{a}_{Y3,H}^{\dagger} \hat{a}_{33,V}^{\dagger} + \hat{a}_{X1,H}^{\dagger} \hat{a}_{1,V}^{\dagger} \hat{a}_{Y1,H}^{\dagger} \hat{a}_{2,V}^{\dagger} \hat{a}_{31,H}^{\dagger} \hat{a}_{32,V}^{\dagger} \hat{a}_{13,V}^{\dagger} \hat{a}_{23,V}^{\dagger} \hat{a}_{Z3,H}^{\dagger} \\
& \quad \left. + \hat{a}_{X1,H}^{\dagger} \hat{a}_{1,V}^{\dagger} \hat{a}_{Y1,H}^{\dagger} \hat{a}_{2,V}^{\dagger} \hat{a}_{Z1,H}^{\dagger} \hat{a}_{3,V}^{\dagger} \hat{a}_{13,V}^{\dagger} \hat{a}_{23,V}^{\dagger} \hat{a}_{33,V}^{\dagger} \right)
\end{aligned} \tag{D6}$$

For example, if we postselect the cases when a photon arrives at the upper-most detector in each subtractor, the final state becomes

$$\frac{1}{\sqrt{5}} \left(\hat{a}_{11,H}^{\dagger} \hat{a}_{21,H}^{\dagger} \hat{a}_{31,H}^{\dagger} + \hat{a}_{1,V}^{\dagger} \hat{a}_{21,H}^{\dagger} \hat{a}_{31,H}^{\dagger} + \hat{a}_{1,V}^{\dagger} \hat{a}_{21,H}^{\dagger} \hat{a}_{3,V}^{\dagger} + \hat{a}_{1,V}^{\dagger} \hat{a}_{2,V}^{\dagger 2} \hat{a}_{31,H}^{\dagger} + \hat{a}_{1,V}^{\dagger} \hat{a}_{2,V}^{\dagger 2} \hat{a}_{3,V}^{\dagger} \right) |vac\rangle \tag{D7}$$

The success probability is $5/(3^{2 \cdot 2^7})$ with feed-forward.